Colloid Polym Sci (2002) 280:438–445
DOI 10.1007/s00396-001-0630-7

ORIGINAL CONTRIBUTION

Tsuneo Okubo
Akira Tsuchida

Structural and dynamic properties of colloidal liquids and gases of silica spheres (29 nm in diameter) as studied by the light scattering measurements

Received: 14 September 2001
Accepted: 7 November 2001

T. Okubo (✉) · A. Tsuchida
Department of Applied Chemistry and
Graduate School of Materials Science
Gifu University, Gifu 501–1193, Japan
E-mail: okubotsu@apchem.gifu-u.ac.jp

Abstract Static and dynamic light-scattering measurements are made for colloidal-liquids and -gases of silica spheres (29 nm in diameter) in the exhaustively deionized aqueous suspension and in the presence of sodium chloride. Single broad peak is observed in the light-scattering curve and the liquid-like and gas-like distributions have been observed. Colloidal crystals are not formed at any sphere concentrations. The nearest-neighbored interparticle distances of colloidal liquids, l_{obs}, agree excellently with the effective diameters of spheres (d_{eff}) including the electrical double layers in the effective soft-sphere model and also with the mean intersphere distances, l_o, calculated from the sphere concentration, i.e., $l_{obs} \approx d_{eff} \approx l_o$. This relation supports the importance of the electrostatic interparticle repulsive interaction. Two dynamic processes have been extracted separately from the time profiles of autocorrelation function of colloidal liquids. Decay curves of colloidal gases are characterized by the single translational diffusion coefficients, which are always lower than the calculation from the Stokes-Einstein equation using true diameter of spheres and increase as ionic concentration increases. These experimental results emphasize the importance of the expanded electrical double layers and the electrostatic intersphere repulsion on the structural and dynamic properties of the colloidal liquids and gases.

Keywords Light scattering · Colloidal liquids · Colloidal gases · Colloidal silica spheres

Introduction

Colloidal suspensions display the extraordinary structures in particle distribution, such as crystal-like distributions especially in the deionized state [1, 2, 3, 4, 5, 6]. This structural peculiarity has been explained mainly with the extended electrical double layers formed around the particles and the electrostatic interparticle repulsion [1, 2, 3, 4, 5, 6, 7, 8, 9, 10, 11, 12, 13, 14, 15, 16].

Ionic groups either dissociated or adsorbed on the colloidal surfaces leave their counterions in suspension, and these excess charges accumulate near the surface forming an *electrical double layer*. The counterions in the diffuse region in the double layer are distributed according to a balance between the thermal diffusive forces and the forces of electrical attraction with colloidal particles. The thickness of the double layers is approximated with the Debye-screening length (l_{DH}):

$$l_{DH} = \left(4\pi^{e^2} n / k_B \epsilon T\right)^{-1/2}, \qquad (1)$$

where e is the electronic charge, ϵ is the dielectric constant of the solvent, k_B is the Boltzmann constant, and n is the concentration of free-state cations and anions in suspension, and is given by $n = n_c + n_s + n_o$, where n_c is the concentration (number of ions per cm^3) of diffusible counterions, n_s is the concentration of foreign salt, sodium chloride in this work, and n_o is the concentration of both H^+ and OH^- ions from the dissociation of water. In order to estimate n_c, the fraction of free counterions (β) must be known, since most counterions are bound tightly with the ions of the colloidal surface [7, 17, 18, 19, 20]. Note that β of silica spheres is estimated to be 0.1 [19, 20] and the largest value of l_{DH} is ca. 1 μm in water.

According to the effective soft-sphere model [21, 22, 23, 24, 25, 26, 27], which is a simple but very convenient assumption especially for the *deionized* colloidal suspension, crystal-like ordering is formed when the effective diameter (d_{eff}) of the spheres including the Debye-screening length is close to or larger than the intersphere distance (l), i.e., d_{eff} [=diameter $(d_o)+ 2\times l_{DH}] > l$. In crystal-like structures, the spheres fluctuate around their equilibrium positions. When d_{eff} is comparable to or shorter slightly than the l value, the distribution of the spheres is usually liquid-like and the spheres move with translational diffusion, though the effective concentration is higher than the stoichiometric concentration due to the extended electrical double layers. When d_{eff} is much shorter than l, a gas-like distribution is observed. Note that the observed intersphere spacing (l_{obs}) is always close to the calculated mean intersphere distance (l_o), and l_o can be safely replaced with l.

It should be noted here that the electrical double layers may not be formed firmly when the sphere size is not large enough compared with the simple ions, since the small spheres move very vigorously by Brownian motion. It is highly plausible that the critical concentration of crystallization of colloidal spheres depends mainly on the mean sphere size and the monodispersity of the spheres, though other factors such as suspension temperature, viscosity and dielectric constant of solvent, and charge density of spheres are also important. When highly polydispersed spheres are used, the sphere distribution comes to be amorphous-solid instead of crystal-like [28]. From our experiences, the spheres smaller than 50 nm in diameter did not form crystal-like structure in the exhaustively deionized and diluted suspensions [29, 30]. However, this critical size will decrease further in future when the monodispersity of the spheres is improved greatly. One of the main purposes of this work is to check whether the colloidal spheres of 29 nm in diameter form crystal-like distribution or not in deionized suspension.

Difference in distribution between the crystal-like and liquid-like is clear when the structure factor, $S(q)$ term is derived from the scattering curves and the theory on the particle form factor, $P(q)$. For colloidal crystals very sharp peaks, which are well assigned to the respective lattice planes, appear. On the other hand, $S(q)$ term of the colloidal liquids shows the single broad peak or multiple sharp peaks (their intensities decrease rapidly from the primary to secondary, tertiary, continuously) for disordered and ordered liquids, respectively [31]. It is interesting to note here that the dynamic modes of fluctuation of spheres at the liquid-crystal transition region do not differ between them so much [31]. In particular, the synchronous mode of the translational movement of spheres plays an important role for the structure formation of liquid and crystal structures similarly. Another interest of this work is to clarify the structural and dynamic nature of the liquid-like structure of small colloidal spheres.

Static (SLS) and dynamic light scattering (DLS) techniques are known as ones of the most precise methods for determining sphere diameter and are also suitable for study of dynamics of interacting particle systems [32, 33, 34, 35, 36, 37, 38, 39, 40, 41]. However, several researchers including us have experienced that the diameter of colloidal spheres estimated by the DLS method is often a bit larger (within 10% in most cases) than that obtained from electron microscopy. This difference has often been beyond the extent explainable by the shrinking of spheres in the course of drying for the latter technique, and should be related to the significant role of the electrical double layers formed around the colloidal particles. Several years ago we reported the extraordinary translational-diffusion behavior of colloidal spheres in deionized suspension by using a metallurgical microscope [42]. The translational self-diffusion coefficients of polystyrene spheres, 120 nm in diameter, decreased sharply as NaCl concentration decreased. We also found that the rotational diffusion coefficients of ellipsoidal colloids of tungstic acid [43, 44] and poly(tetrafluoroethylene) [45] colloids decreased as the ionic concentration of suspension decreased. These observations have been interpreted in terms of the extended electrical double layers. This work also aims to clarify the role of the electrical double layers on the translational diffusion of colloidal particles in the gas-like state.

Experimental

Materials. Colloidal silica spheres of CS22P was a gift from Catalyst & Chemicals Ind. Co. (Tokyo). Diameter (d_o), standard deviation (s) from the mean diameter, and polydispersity index (s/d_o) were 29 nm, 6 nm, and 0.21, respectively. d_o and s were determined from an electron microscope. The charge density of the spheres was determined by conductometric titration with a Wayne-Kerr autobalance precision bridge, model B331, mark II (Bognor Regis, Sussex). Charge density of strongly acidic groups was 0.48 μC/cm^2. The sphere sample was carefully purified several times using an ultrafiltration cell (model 202, membrane: Diaflo-XM300, Amicon Co.). Then the sample was treated on a mixed bed of cation- and anion-exchange resins [Bio-Rad, AG501-X8 (D), 20–50 mesh] more than one year before use, since the newly produced silica spheres release a considerable amount of alkali ions from sphere surfaces for a long time. Water used for the purification and for suspension preparation was purified by a Milli-Q system (Milli-RO5 plus and Milli-Q plus, Millipore Co., Bedford, MA).

Static (SLS) and dynamic light-scattering (DLS) measurements. The SLS and DLS measurements were performed on a dynamic light scattering spectrophotometer (type DLS-7000, Otsuka Electronics, Osaka). The sample of 5 ml was prepared by filtering with a disposable syringe filter unit (DISMIC-25, 0.2 μm, Toyo Roshi Co. Tokyo) into a Pyrex cylindrical cell (12 mm in outside diameter and 130 mm in length) with a screw cap. These cylindrical cells were ground carefully to a spectroscopic guaranteed level. SLS and DLS measurements for the samples without resins were made within 2 h after the suspension was set in the cells. However, measurements for the *deionized* suspensions with the Bio-Rad resins were made *more than three or four weeks* after the suspension was set. Amount of the resins was always much in excess compared with the ionic impurities in suspension. Absorption of the colloidal spheres on the resins was safely neglected by the repeated mixing of the suspension. Note that it takes so long before attaining the *completely deionized* suspension with the coexistence of the ion-exchange resins. During the measurement the cuvette was kept under isothermal conditions at 24 ± 0.02 °C in a cylindrical vat containing silicon oil.

Data analysis was made with the cumulant and histogram methods including non-negative least square (NNLS) analysis [46]. The autocorrelation function of the scattered light, $g^{(1)}(\tau)$, where τ is the correlation time, is actually found to be a single exponential function only for the suspension containing foreign salt and/or gas-like structures. For liquid-like suspensions the intersphere interaction is so strong that $g^{(1)}(\tau)$ deviates greatly from a single exponential. In these cases NNLS analysis was applied in this work in order to obtain the distribution of the decay rates, and then the diffusion coefficients [46].

Here, we describe briefly the basic equations for the light scattering measurements [40, 47, 48]. The homodyne photon-correlation spectroscopy measures the intensity auto-correlation function $g^{(2)}(\tau)$ which is related to $g^{(1)}(\tau)$ following the Gauss central-limit theorem:

$$g^{(2)}(\tau) = 1 + \beta\left|g^{(1)}(\tau)\right|^2 \tag{2}$$

where β is the amplitude. When the suspension of monodispersed spheres is sufficiently dilute so that the inter-sphere interaction may be negligible, the decay of concentration fluctuation occurs by the translational diffusion motion of a free particle. The $g^{(1)}(\tau)$ is represented by a single exponential type of decay function, Eq. (3), from which the translational diffusion coefficient, D_o is easily estimated:

$$g^{(1)}(\tau) = \exp\left(-q^2 D_0 \tau\right) \tag{3}$$

where q is the scattering vector whose magnitude is equal to $(4\pi n_r/\lambda)\sin(\theta/2)$ where λ is the wavelength of the incident beam in medium, θ is the scattering angle, and n_r is the refractive index of solvent.

In the liquid-like state where the colloidal particles are locally ordered to be reflected as the maximum of the static structure factor $S(q)$ at q_m, $g^{(1)}(\tau)$ is no more fitted by Eq. (3). In this case, the first cumulant $\Gamma_e \equiv K_1$ defined by Eq. (4) is conveniently used for characterization of dynamical behavior of the spheres in the liquid state:

$$\ln g^{(1)}(\tau) = \sum K_n(-\tau)^n/n! \tag{4}$$

where the K_n terms are the n-th order cumulants. The Γ_e was found proportional to $S(q)^{-1}$ as predicted by the theory. For $q \gg q_m$ $S(q) \cong 1$; on the other hand, $g^{(1)}(\tau)$ shows the bimodal distribution of the decay rate, in which the short time diffusion coefficient is close to D_o and the long time diffusion coefficient D_l is smaller than D_o by a factor of about 3 [47]. The short time behavior represents the Brownian motion of the particle in a cage formed by neighboring particles, and the behavior at the long time end (much) longer than the lifetime of the cage, τ_I, according to the notation by Pusey, represents diffusion through several nearest-neighbor cages.

Results and discussion

Light-scattering curves

Figure 1 shows the light-scattering intensity, $I(q)$ as a function of scattering vector, q for the suspensions with resins, without resins and in the presence of sodium chloride. The scattering curves for the suspensions with and without resins showed a broad peak. This indicates that the suspensions are "disordered" liquid-like, i.e., typical structure of liquids. The disordered liquids gave the single peak only. These curves with resins showed rather sharp peaks compared with those without resins. However, the distribution was again disordered liquid-like [31]. By the addition of sodium chloride the structure transformed from liquid-like to gas-like distributions.

Structure factor, $S(q)$ of colloidal liquids

For colloidal suspension of spherical particles the structure factor $S(q)$ shows the particle distribution more accurately than $I(q)$. The peaks in the scattering curve of colloidal liquids are broad and the background

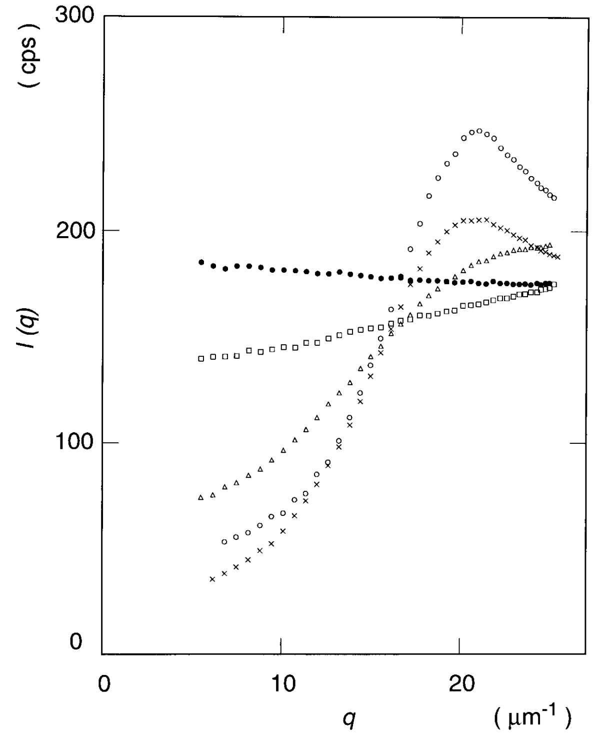

Fig. 1 Scattering intensity of the suspensions of CS22P spheres as a function of scattering vector at 24 °C. $\phi = 0.000392$, *open circles*: with resins, *crosses*: without resins, *open triangles*: [NaCl] = 0.000014 mol/l, *open squares*: 0.00006 mol/l, *filled circles*: 0.0008 mol/l

intensity is high so that there should be difference between the profiles in the structure factor and in the intensity of scattered light. $I(q)$ is given by

$$I(q) \propto P(q)S(q) \tag{5}$$

where $P(q)$ is the particle structure (form) factor and can be estimated experimentally from the $I(q)$ measurements on the same suspension but in the presence of salt, for example. For spherical particles $P(q)$ has been given as Eq. (6) theoretically [49]:

$$P(q) = \left\{3[\sin(qd_0/2) - (qd_0/2)\cos(qd_0/2)]/(qd_0/2)^3\right\}^2 \tag{6}$$

Using the observed $I(q)$ and Eq. (6), $S(q)$ vs q curves are obtained for all the sample suspensions.

Figure 2 shows the $S(q)$ curves for the suspensions without resins. Clearly, the distribution at $\phi = 0.0000261$ was gas-like and other suspensions of higher sphere concentrations were liquid-like, especially "disordered liquid". The magnitudes of $S(q_m)$ were between unity and 1.3, where q_m denotes the peak scattering vector.

Figure 3 shows the $S(q)$ curves for the deionized suspensions with the resins. In these cases, all the suspensions were liquid-like. Figure 4 shows the $S(q)$ curves for the suspensions with and without resins, and further in the presence of sodium chloride. The peak wavelengths obtained from this figure increased slightly as the ionic concentration of the suspension increases.

Figure 5 compares l_{obs}, l_o, and d_{eff} values. Clearly, the relation $l_{obs} = l_o \le d_{eff}$ holds. Thus, these relations definitely support the importance of the electrostatic intersphere repulsion and the validity of the effective soft-sphere model described in the introduction.

Time dependence of the diffusion coefficients after suspension was set with ion-exchange resins

Diffusion coefficients of two suspensions were determined from the cumulant and NNLS analyses as a function of time passed after suspensions were set with the resins in Fig. 6a,b. In Fig. 6a, the suspension structures within 15 days were gas-like, since the diffusion coefficients from the cumulant and NNLS methods were quite similar to each other. After 19 days, however, two kinds of D-values, larger and smaller ones compared with those from the cumulant analysis, were evaluated by the NNLS method, which demonstrates the liquid-like nature of suspension. This observation

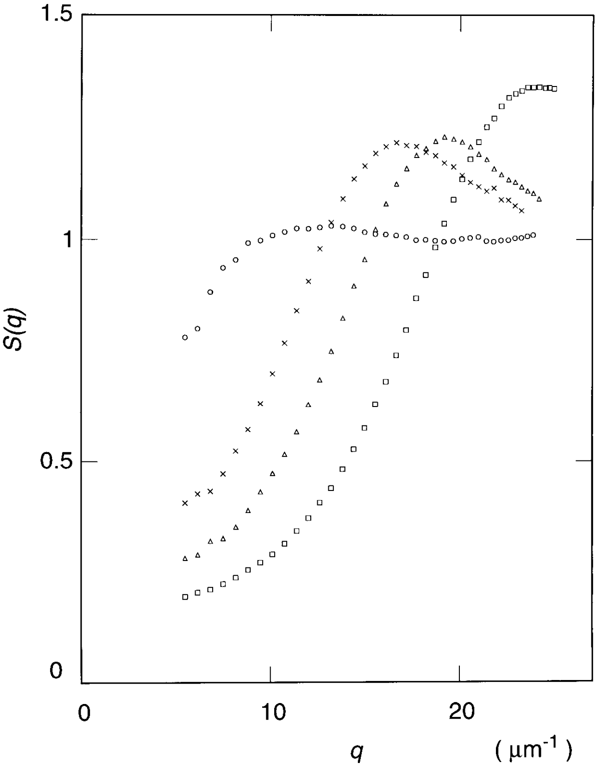

Fig. 2 $S(q)$ of the suspensions of CS22P spheres as a function of scattering vector at 24 °C. Without resins, *open circles*: $\phi = 0.0000261$, *crosses*: 0.000157, *open triangles*: 0.000261, *open squares*: 0.000522

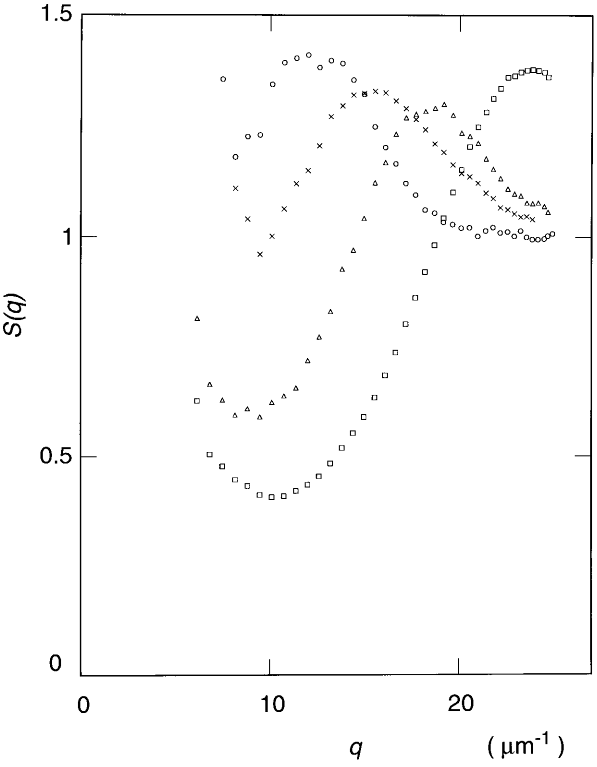

Fig. 3 $S(q)$ of the suspensions of CS22P spheres as a function of scattering vector at 24 °C. With resins, *open circles*: $\phi = 0.0000783$, *crosses*: 0.000157, *open triangles*: 0.000261, *open squares*: 0.000522

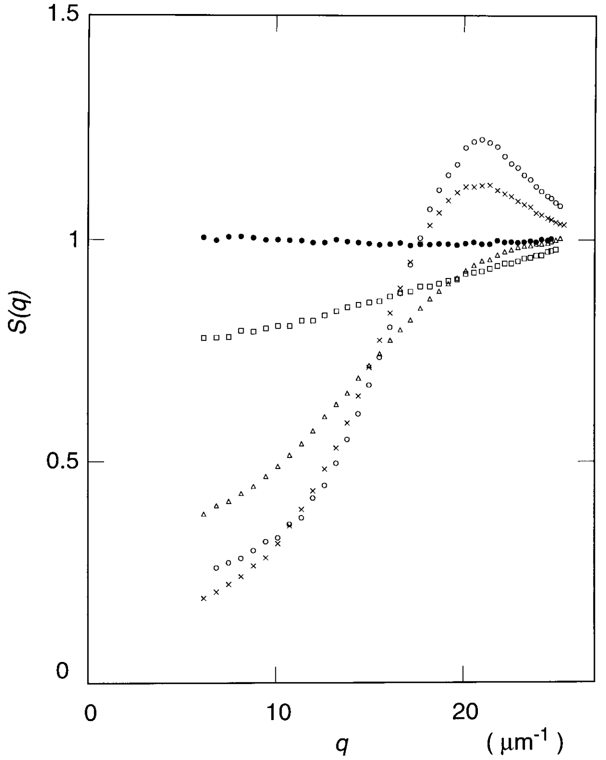

Fig. 4 $S(q)$ of the suspensions of CS22P spheres as a function of scattering vector at 24 °C. $\phi = 0.000392$, *open circles*: with resins, *crosses*: without resins, *open triangles*: [NaCl] = 0.000014 mol/l, *open squares*: 0.00006 mol/l, *filled circles*: 0.0008 mol/l

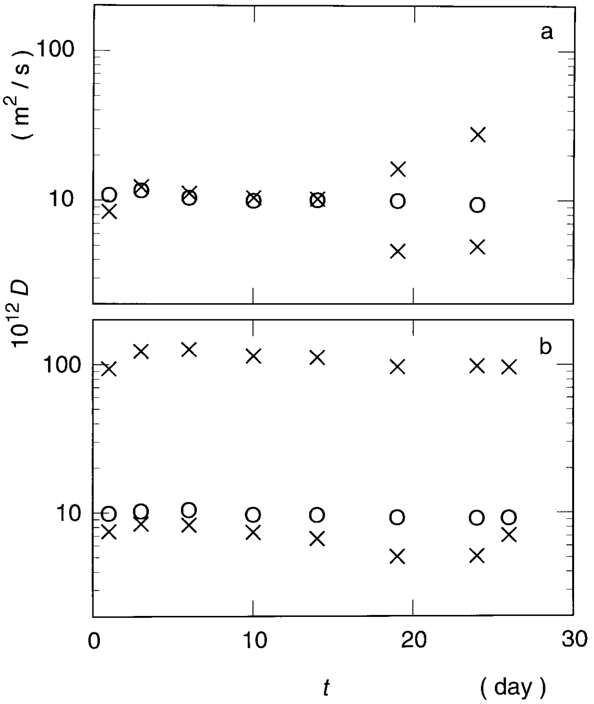

Fig. 6a,b Diffusion coefficients of CS22P spheres as a function of time passed after setting the sample with resins at 24 °C: **a** $\phi = 0.0000783$; **b** $\phi = 0.00261$. *Open circles*: cumulant analysis, *crosses*: NNLS analysis. $\theta = 90°$

confirms that the deionization reaction of sphere suspension with the Bio-Rad resins takes a long time, two to three weeks before the exhaustively deionized state is attained. This will be due to the fact that the deionization reaction is consecutive and takes place between solid and liquid phases, i.e., between ionic groups at the surfaces of colloidal spheres in the solid phase and liquid phase, and between the liquid-phase and the charge groups of ion-exchange resins in the solid phase. Transformation between the gas-like and liquid-like structures is substantially faster compared with the deionization reaction.

When the sphere concentration is much higher compared with the critical concentration of melting, the suspension structure remains liquid-like at the beginning stage of suspension set as is clear in Fig. 6b.

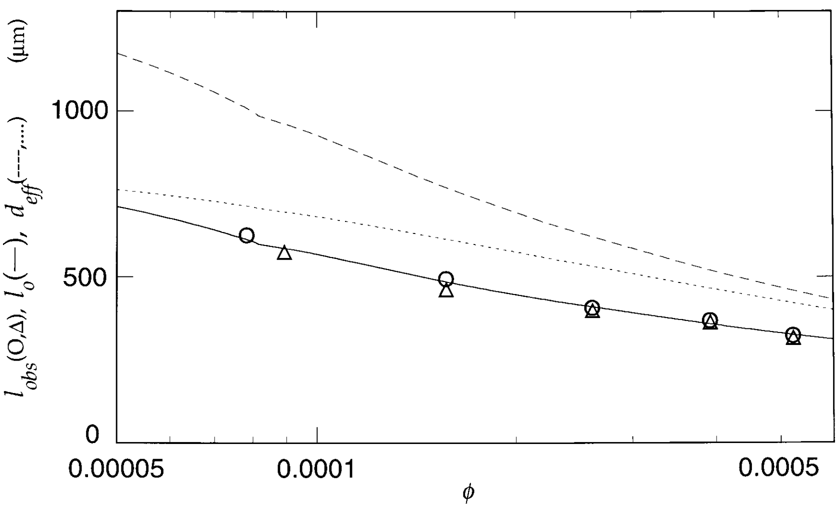

Fig. 5 Comparison of l_{obs} (*open circles*: with resins, *open triangles*: without resins), l_o (*solid curve*) and d_{eff} (*broken curve*: with resins, *dotted curve*: without resins) for the suspensions of CS22P spheres

Dynamic character of colloidal liquids and gases

Time profile of the light intensity auto-correlation function, $g^{(2)}(\tau)$ of the colloidal liquids of CS22P spheres deviated greatly from the calculated value from cumulant analysis of the unimodal distribution of the decay rates, though the graph showing this was omitted. This kind of deviation supports the idea that there exist multi modes for the colloidal liquids. Separation into multi modes from the auto-correlation function was performed mainly by the histogram analysis of the nonnegative least square (NNLS) method and occasionally by the Marquadt method, when we need to ascertain the validity of the peak separation with the former analysis.

Figure 7a,b shows the sphere concentration dependencies of the diffusion coefficients with and without resins obtained from data analysis with the cumulant method (shown by open circles) and also with the NNLS method (shown by crosses). The liquid-like structure was characterized by the short time (D_s) and long time diffusion coefficients (D_l) with $D_s = D_o$ and $D_l \cong D_s/3$.

In the presence of excess amount of sodium chloride the diffusion coefficients evaluated from the cumulant and NNLS analyses agreed with each other and also with those estimated from Stokes-Einstein equation, though the graphs showing this are omitted here. The suspension was gas-like. With resins the suspension structures were liquid-like. Without resins the suspensions of concentrations lower than $\phi = 0.0001$ showed gas-like distribution. Structure transformed to liquid-like above ca. $\phi = 0.0001$. Addition of 10^{-5} mol/l of sodium chloride does not affect the suspension structure so much, but the gas-like distribution was observed below $\phi = 0.0002$. In the presence of rather high concentrations of sodium chloride the sphere distribution was gas-like irrespective of sphere concentrations up to 0.003 in volume fraction.

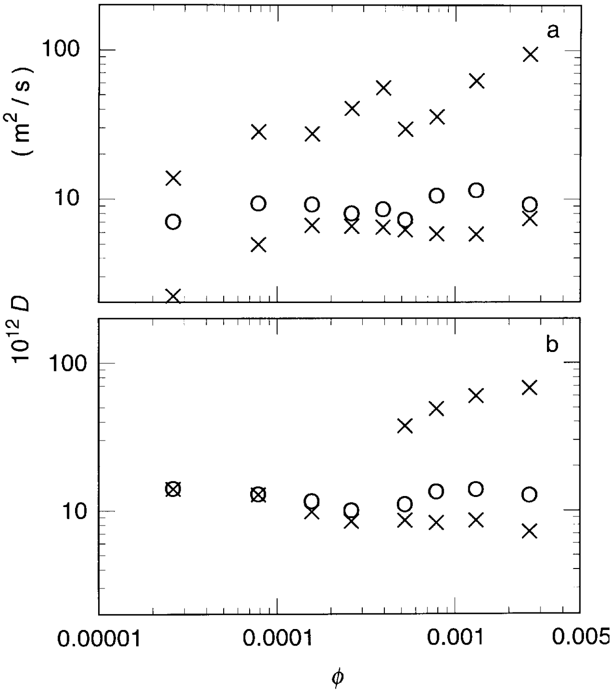

Fig. 7a,b Diffusion coefficients of CS22P spheres as a function of sphere concentration at 24 °C: **a** with resins; **b** without resins. *Open circles*: cumulant analysis, *crosses*: NNLS analysis

The diffusion coefficients for the suspensions showing sharp peaks in the light-scattering curve were substantially low. Furthermore, the background D-values increased as the scattering vector increased, whereas the background intensity of scattered light decreased as q increased. According to Pusey and Tough [36], the first cumulant K_I in Eq. (4) is given by

$$K_I = D_0 q^2 / S(q) \qquad (7)$$

where D_o is the diffusion coefficient for a system of non-interacting particles. Thus, the "effective diffusion coefficient", D_{eff} is given by

$$D_{eff} = D_0 / S(q) \qquad (8)$$

Constancy of D_{eff} x $S(q)$ has been satisfactory for the colloidal liquids [36, 50, 51]. Comparison of $S(q)$ values in Fig. 4 and D_{eff} values observed confirms that Eq. (8) is also valid for the colloidal crystals, when we take into account the experimental errors in two parameters and the logarithm plots for the D-values where the q dependence in the range of small D values is emphasized. Quite similar features have been obtained for the suspensions with and without resins at $\phi = 0.000159$, though the figures demonstrating this were also omitted here.

Dynamic character of colloidal gases

Figure 8 shows the salt concentration dependence of the effective diffusion coefficient, D_{eff} in the presence of sodium chloride, in the absence and presence of ion-exchange resins. In the presence of salt above ca. 0.00006 mol/l, D_{eff} agreed with the translational diffusion coefficient D_o, and the suspension structure was gas-like. Clearly, D_{eff}-values decreased as salt concentration increased. The most impressive feature in this figure is that D_{eff} increased significantly by 68% as concentration of sodium chloride increased. This change is explained in terms of thinning of the electrical double layers with increasing ionic concentration of suspension. Good agreement between the experiment and the calculation from the d_{eff}-values is attained especially at high concentrations of sodium chloride. The important contribution of the electrical double layers is clear. This salt influence on the diffusion behavior strongly confirms

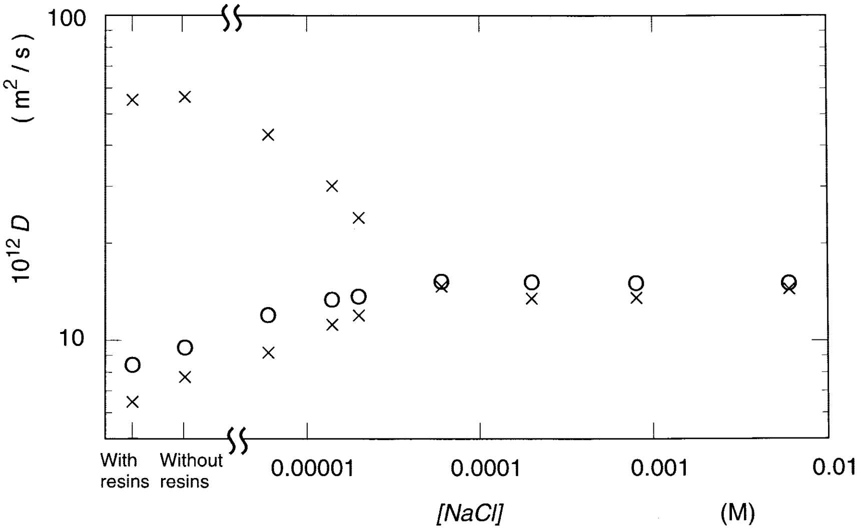

Fig. 8 Diffusion coefficients of CS22P spheres as a function of ionic concentration at 24 °C. $\phi = 0.000392$. *Open circles*: cumulant analysis, *crosses*: NNLS analysis

that the colloidal spheres are always accompanied with the electrical double layers and the translational movement of the former is retarded as the latter expands.

Acknowledgments A dynamic light-scattering spectrophotometer was purchased by a grant-in-aid from the Mitsubishi Foundation, to whom this author thanks sincerely. Catalyst & Chemicals Ind. Co. (Tokyo) is appreciated deeply for kindly providing colloidal silica samples. The Ministry of Education, Culture, Sports, Science and Technology, Japan is also thanked for grants-in-aid for Scientific Research on Priority Area (A) (11167241). Professor Norio Nemoto of Kyushu University is acknowledged deeply for his valuable discussion on this work. T. O. sincerely thanks the late Professor emeritus Sei Hachisu of Tsukuba University for his interest and encouragement through this work.

References

1. Kose A, Ozaki M, Takano K, Kobayashi Y, Hachisu S (1973) J Colloid Interface Sci 44:330
2. Pieranski P (1983) Contemp Phys 24:25
3. Ottewill RH (1985) Ber Bunsenges Phys Chem 89:517
4. Aastuen DJW, Clark NA, Cotter LK, Ackerson BJ (1986) Phys Rev Lett 57:1733
5. Pusey PN, van Megen W (1986) Nature (London) 320:340
6. Okubo T (1988) Acc Chem Res 21:281
7. Vanderhoff W, van de Hul HJ, Tausk RJM, Overbeek JTG (1970) In: Goldfinger G (ed) Clean surfaces: their preparation and characterization for interfacial studies. Dekker, New York, p 15
8. Hiltner PA, Papir YS, Krieger IM (1971) J Phys Chem 75:1881
9. Williams R, Crandall RS, Wojtowicz PJ (1976) Phys Rev Lett 37:348
10. Mitaku S, Ohtsuki ST, Enari K, Kishimoto A, Okano K (1978) Jpn J Appl Phys 17:305
11. Lindsay HM, Chaikin PM (1982) J Chem Phys 76:3774
12. Robbins MO, Kremer K, Grest GS (1988) J Chem Phys 88:3286
13. Rundquist PA, Photinos P, Jagannathan S, Asher SA (1989) J Chem Phys 91:4932
14. Monovoukas Y, Gast AP (1991) Langmuir 7:460
15. Sood AK (1991) Solid State Phys 45:2
16. Okubo T (1993) Prog Polymer Sci 18:481
17. Schaefer DW (1977) J Chem Phys 66:3980
18. Alexander S, Chaikin PM, Grant P, Morales GJ Pincus P, Hone D (1984) J Chem Phys 80:776
19. Okubo T (1987) Ber Bunsenges Phys Chem 91:1064
20. Okubo T (1988) J Colloid Interface Sci 125:380
21. Baker JA, Henderson D (1967) J Chem Phys 47:2856
22. Wadachi M, Toda M (1972) J Phys Soc Jpn 32:1147
23. Hachisu S, Kobayashi Y, Kose A (1973) J Colloid Interface Sci 42:342
24. Brenner SL (1976) J Phys Chem 80:1473
25. Takano K, Hachisu S (1977) J Chem Phys 67:2604
26. Barnes CJ, Chan DY, Everett DH, Yates DE (1978) J Chem Soc Faraday Trans 274:136
27. Voeglli LP, Zukoski CF IV (1991) J Colloid Interface Sci 141:79
28. Okubo T (1990) Colloid Polymer Sci 268:1159
29. Okubo T (1987) J Chem Phys 87:3022
30. Okubo T (1994) Langmuir 10:1695
31. Okubo T, Kiriyama K (1996) Ber Bunsenges Phys Chem 100:849
32. Batchelor GK (1972) J Fluid Mech 52:245
33. Ohtsuki T, Okano K (1982) J Chem Phys 77:1443
34. Belloni L, Drifford M (1985) J Phys Lett 46:1183
35. Beresford-Smith B, Chan DYC, Mitchel DJ (1985) J Colloid Interface Sci 105:216
36. Pusey PN, Tough RJA (1985) In: Pecora R (ed) Dynamic light scattering. Plenum, London
37. Russel WB, Saville DA, Schowalter WR (1989) Colloidal dispersions. Cambridge Univ. Press, Cambridge
38. Cichocki B, Felderhof BU (1991) J Chem Phys 94:556
39. Denkov ND, Petsev DN (1992) Physica A 183:462
40. Okubo T, Kiriyama K, Nemoto N, Hashimoto H (1996) Colloid Polymer Sci 274:93
41. Okubo T, Kiriyama K (1997) J Mol Liquids 72:347
42. Okubo T (1989) J Phys Chem 93:4352
43. Okubo T (1987) J Am Chem Soc 109:1913

44. Okubo T, Tsuchida A, Yoshimi H, Maeda H (1999) Colloid Polymer Sci 277:601
45. Okubo T, Shimizu T (1990) J Colloid Interface Sci 135:300
46. Lawson CL, Hanson RJ (1974) Solving least squares problems. Prentice-Hall, New Jersey
47. Schatzel K, Ackerson BJ (1993) Phys Rev E 48:3766
48. Pusey PN (1978) J Phys A Math Gen 11:119
49. Berne B, Pecora R (1980) Dynamic light scattering. Plenum, New York
50. Dalberg PS, Boe A, Strand KA, Sikkeland T (1978) J Chem Phys 69:5473
51. Grunner F, Lehmann W (1980) In: Degiorgio V, Corti M, Giglio M (eds) Light scattering in fluids and macromolecular solutions. Plenum, New York